Desalination and Water Treatment
www.deswater.com

doi: 10.5004/dwt.2021.27887

243 (2021) 262–274
December

Performance studies of indigo dye removal using TiO_2 modified clay and zeolite ultrafiltration membrane hybrid system

Mohamed Romdhani[a,b], Wala Aloulou[a], Hajer Aloulou[a], Catherine Charcosset[b], Samia Mahouche-Chergui[c], Benjamin Carbonnier[c], Raja Ben Amar[a,*]

[a]*Chemistry Department, Faculté des Sciences de Sfax, Univ. Sfax, BP1171, 3000 Sfax, Tunisia, emails : benamar.raja@yahoo.com (R. Ben Amar), med594268@gmail.com (M. Romdhani), walaaloulou6@gmail.com (W. Aloulou), hajer.aloulou89@yahoo.fr (H. Aloulou)*
[b]*Univ. Lyon, Université Claude Bernard Lyon 1, CNRS, LAGEP UMR 5007, 43 Boulevard du 11 Novembre 1918, F-69100, Villeurbanne, France, email: catherine.charcosset@univ-lyon1.fr (C. Charcosset)*
[c]*Institut de Chimie et des Matériaux Paris-Est (ICMPE), UMR 7182 CNRS, Université Paris-Est, 2 Rue Henri Dunant, 94320 Thiais, France, email: mahouche.samia@gmail.com (S. Mahouche-Chergui)*

Received 1 August 2021; Accepted 3 October 2021

ABSTRACT

Dyes contamination causes serious damages to aquatic life and human health. With the increase in these persistent organic contaminants accumulation around the world, performant environmentally friendly and low-cost materials and techniques are required to protect the ecosystem and humans. In this study, the efficacy of titania-smectite nanocomposites (Sm-TiO_2 NCs) at removing indigo blue (IB) dye was assessed by both batch adsorption and hybrid treatment combining adsorption and ultrafiltration (UF) processes. During the adsorption, the effect of different parameters on IB removal such as dose of Sm-TiO_2, contact time, pH and IB concentration were studied. The optimal conditions were applied for the Sm-TiO_2 during dye removal using adsorption/UF hybrid treatment. At 293 K and pH 2.5, an optimized dose of Sm-TiO_2 (100 mg/L) removed 73% of the IB from a 25 mg/L solution in 240 min with an equilibrium adsorption capacity greater than 180 mg/g. The adsorption of IB dye by Sm-TiO_2 NCs followed the Langmuir adsorption isotherm model and pseudo-second-order kinetics. The thermodynamic studies revealed that the adsorption process was spontaneous and exothermic. When a hybrid process was applied, a higher IB removal capacity has been obtained with a lower dose of Sm-TiO_2 compared to the case of the batch adsorption process. In addition, the presence of Sm-TiO_2 NCs has been found to reduce the UF membrane fouling. In this case, the adsorption followed by UF treatment applied in two stages was modified to a single-stage hybrid process. Permeate flux was increased from 71 L/h m^2 (only UF) to 182 L/h m^2 (Sm-TiO_2/UF).

Keywords: Indigo blue; Titania-smectite nanocomposites; Adsorption; Ultrafiltration; Hybrid process

1. Introduction

Water, a valuable and necessary component of life, covers 71% of the earth's surface with 97.5% salt water and 2.5% freshwater containing just 0.007% usable for the purpose of drinking [1]. The quality of the available part potentially usable by humans continues to deteriorate and sometimes irreversibly. Among the industrial sectors, the textile industry which usually uses dyes and a variety of chemical additives [2,3], is one of the largest consumers of water in the various treatment operations, producing significant amounts of polluted wastewater.

On another hand, the majority of industrial effluents are not adequately treated, resulting in substantial water

* Corresponding author.

1944-3994/1944-3986 © 2021 Desalination Publications. All rights reserved.

contamination. In particular, colored effluents contain high levels of dyes and other harmful substances, posing a major threat to drinking water quality and causing an adverse effect on soil fertility and fauna and flora environments [4]. Dyes have been shown in recent studies to be toxic and carcinogenic [5–7]. Mittal [7] reported that artificial dyes cause serious side effects, such as hyperactivity in children as well as cancer and allergies. So far, various treatment processes based on physical, chemical and biological techniques have been the subject of extensive research over the last few decades [8–10]. Photocatalytic degradation, oxidation, coagulation–flocculation, membrane filtration and adsorption have all been identified as techniques for textile wastewater treatment. However, because of its removal efficiency, ease of implementation, operational simplicity and low cost, the adsorption process is of great interest in water and wastewater treatment [11,12]. Many adsorbents, such as activated carbon, bio-wastes, zeolite and especially clay materials have been identified to treat dye-contaminated waters [13]. In this way, Mittal et al. [14] observed that activated bottom ash and activated de-oil soya adsorbents exhibit good efficiency for indigo carmine dye removal at a pH range of 2–3 under all the temperatures, while the equilibrium was attained at a contact time of 2–2.5 h and 3–4 h, respectively.

Nanoscale adsorbents are also often used due to the large surface area and uniform sizes of their pores. They usually have different forms of nanocomposites, nanofibrous and magnetic nano-adsorbents [15,16].

Clay and clay–clay-based composite materials were found to be highly efficient adsorbents and present many advantages over other adsorbents since they are readily available, non-toxic, exhibit large surface area (and thus a high number of active sites) and relatively high porosity, a high sorption potential and low cost, which make them excellent candidates for the adsorption and elimination of toxic pollutants from wastewater streams [17]. For example, Chang et al. [18] studied the adsorption of methylene blue (MB) onto Fe_3O_4/activated montmorillonite NC. At 293 K and a pH of 7.37, the Fe_3O_4/Mt nanocomposite (NC) (500 mg/200 mL) removed 99.47% of the MB from a 120 mg/L solution in just 25 min. The authors concluded that the Fe_3O_4/Mt NC had good stability and reusability. Indeed, identical removal rates were obtained after five cycles. For the removal of Pb(II) from aqueous solutions, Msaadi et al. [19] used the montmorillonite/mercaptosuccinic acid material as an adsorbent. For an equilibrium time of 80 min, the maximum adsorption was found to be 74.7 mg/g. The authors confirmed that the activated clay by UV-triggered thiol-ene reaction was suitable to remove a toxic heavy metal ion from aqueous solutions.

The adsorption can be performed in the batch system or using a fixed-bed adsorption column. The choice of the mode of adsorption depends in general on adsorption properties (mesoporosity, surface area, uniformity of pore size [20].

At the same time, the development of low-cost membranes from natural clays has got a lot of attention during the last decade, mainly due to their ability to satisfy separation requirements in a variety of applications, including wastewater treatment [21]. However, in several areas, the use of one treatment technique remains limited and improvements are needed to enhance some performances including permeability, selectivity, and antifouling [22]. For example, Bhattacharya et al. [23] used a ceramic microfiltration (MF) process alone or in combination with a biosorbent prepared from fruit peels of *Lagerstroemia speciosa* to treat high organic loaded wastewater. They found that the hybrid system revealed a lot of promise for treating and reusing high-loaded organic wastewaters in agricultural activities. Kim et al. [24] found that the use of granular activated carbon as adsorbent combined with MF allows an enhancement of MF performance with 60% pollutants removal against only 30% when using only MF. Interestingly, the combination of membrane filtration combined with the adsorption process increased not only the removal efficiency of the dye and enhanced but also the permeate flux [25]. Adsorption and filtration technologies may be combined in many ways, including the use of adsorption as pretreatment to membrane filtration or in the hybrid system using one step integrating an adsorption unit with membrane filtration [25]. Previous studies revealed that the performances of a membrane/adsorption hybrid system are dependent on the reactor configuration, operating modes, adsorbent dosage, and effluent properties. For example, Hammami et al. [26] used a hybrid method that combined adsorption using powder-activated carbon (PAC) and ultrafiltration (UF) to remove dye (i.e., Acid orange 7) from an aqueous solution. It was found that using the hybrid process, the presence of a small amount of PAC adsorbent reduced UF membrane fouling and PAC dosage while an increase of the permeate flux and an improvement in the dye removal efficiency.

According to the authors' knowledge, a small number of studies related to the hybrid membrane adsorption system have been accomplished. The majority of previous research has primarily concentrated on traditional hybrid systems that are run in a sequential manner.

The present work focuses on the use of Sm-TiO_2 NC as an adsorbent and UF zeolite membrane for the removal of indigo blue (IB) in a hybrid system. Firstly, we are interested in the study of the effects of adsorbent dosage, reaction time, solution pH, initial dye concentration and temperature on the IB removal. Then the adsorption/UF zeolite membrane (Sm-TiO_2/UF) hybrid system applied in different configurations was investigated to determine the optimum configuration and experimental conditions for the best performance to remove IB. For that, the effect of Sm-TiO_2 dose, pH and initial IB concentration on the permeate flux and UF membrane fouling was determined.

2. Materials and methods

2.1. Dye solution

In this work, a novel hybrid clay-TiO_2 NC adsorbent/zeolite UF membrane was used to treat wastewater containing indigo blue (IB) dye ($C_{16}H_{10}N_2O_2$). IB is an organic dye, the most important of indigoid dyes, very useful in the textile industry, especially in the production of jeans (Fig. 1a). It is a dark blue crystalline powder. The latter is insoluble in water and poorly soluble in most common solvents, so it must be reduced to a soluble form (leuco form) through a strong binding agent (sodium hydrosulfite in our case). The composition of the synthetic solution provided by SITEX Company located in Ksar Hellal (Tunisia) is given in Table 1.

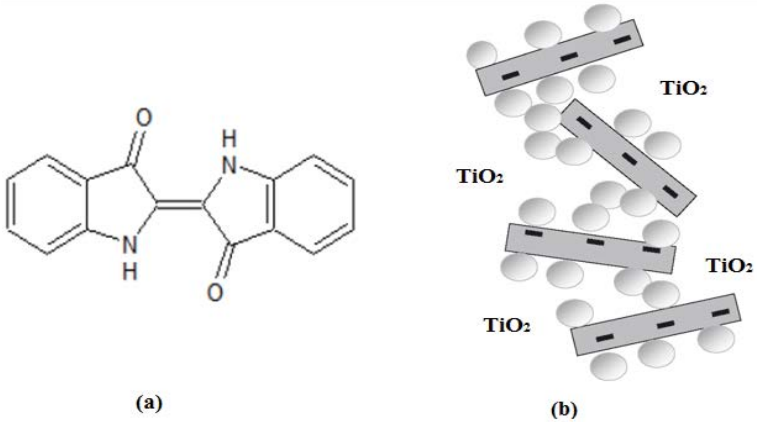

Fig. 1. Materials used: indigo blue dye (a) and schematic representation of Sm-TiO_2 (b).

2.2. Adsorbent

The adsorbent used in this study is smectite-titania-NCs (Sm-TiO_2) prepared from natural clay (Fig. 1b). The smectite was collected from Jebel Stah situated in the west of Gafsa City located in west-central Tunisia. This modified clay was prepared according to the sol–gel method previously reported by Aloulou et al. [27]. The specific surface area (BET), the total pore volume and the mean pore size of the NCs (Sm-TiO_2) are 92 m^2/g and 0.19 cm^3/g and 8–12 nm, respectively. The methods of characterization were detailed previously [27]. Briefly, the total surface area, pore diameter and total pore volume of the Sm-TiO_2 NC were determined using the BET method and probing the solid surface with nitrogen as the gaseous adsorbate. The instrument used was an ASAP 2020 instrument (Micromeritics, France, S.A.R.L).

2.2.1. Fourier-transform infrared spectroscopy study

Fourier-transform infrared spectroscopy (FTIR) spectra were obtained from Sm-TiO_2 before and after adsorption onto IB using a Bruker TENSOR 27 (Bruker Optics Ltd., Coventry, UK) FTIR spectrometer equipped with a diamond attenuated total reflectance module. The measurements were performed in the wavenumber range of 400–4,000 cm^{-1} at 4 cm^{-1} resolution.

2.3. UF membrane

A tubular zeolite UF membrane (pore size of 0.18 μm and water permeability of 534 L/h m^2 bar) previously developed in our laboratory by Aloulou et al. [28] was used in this study. This membrane named Z42/Z was prepared from zeolite (particle size (φ) < 42 μm) layer deposition on support from the same type of material, by the slip-casting method. Further details on the preparation method are given in our previous publication [28]. Membrane permeability was measured using distilled water at a temperature of 25°C and different transmembrane pressure (TMP). A nitrogen gas source was used to maintain the working pressure. The permeability of the Z42/Z membrane was evaluated by varying the distilled water flux J_w (L/h m^2) with TMP (bar) according to Darcy's law as specified by Aloulou et al. [28].

Table 1
Composition of the synthetic solution of indigo blue dye provided by the SITEX Company located in Ksar Hellal (Tunisia)

Composition	*C* (g/L)
Indigo blue	1
Wetting	0.5
Sulfur blue	5
Sodium hydrosulfite	0.5
NaOH	pH = 11
Sequestering	0.1
Softeners	0.3

2.4. Adsorption experiments

A series of IB Dye solutions containing known concentrations were prepared from a stock solution of 1 g/L (Table 1). The tests were performed by adding a known quantity of Sm-TiO_2 in 100 mL of the synthetic solution under stirring with a magnetic stirrer (WiseStir HS-100D, Witeg) at 450 rpm. Batch adsorption studies were carried out by varying the adsorbent dose (10–400 mg), contact time (10–300 min), initial concentration of IB (4–5 mg/L), initial pH (1.5–9) and temperature (293–313 K). After each experiment, the Sm-TiO_2 NC was separated from dye solutions by using a filter paper (0.45 μm). The concentration of IB was obtained by measuring the absorbance on a UV/visible spectrophotometer (Aquanova Jenway, Designed and Manufactured in the UK) at a wavelength of 620 nm. The dye removal efficiency was calculated using Eq. (1):

$$R(\%) = \frac{(C_i - C_e)}{C_i} \times 100 \quad (1)$$

The adsorption capacity of IB dye by NC was determined by Eq. (2):

$$q_e = \frac{(C_i - C_e)}{m} \times V \quad (2)$$

where C_i and C_e are the initial and equilibrium dye concentration (mg/L). V is the volume of the dye solution (L), and m is the weight of the adsorbent (g).

2.5. Adsorption-UF hybrid system

To study the performance of the hybrid system adsorption/UF (Sm-TiO_2/Z42/Z), two configurations were applied. In the first configuration, adsorption was used as a pretreatment step prior to UF. The experimental device operates in recirculation mode, that is, with retentate recycling back to the feed tank and permeate recovery. The permeate flux was measured according to Eq. (3). After each test, the UF membrane was regenerated using a 15 min backflushing technique followed by a 20 min acid (nitric acid 2% at 60°C) and alkaline (2% NaOH at 80°C) treatment. After that, the membrane was rinsed with distilled water until the wash water was pH neutral [28].

$$J = \frac{V}{S \cdot t} \tag{3}$$

where V is the volume of permeate (L), S the membrane area (m^2), t the time (h) and J the permeation flux (L/m^2 h).

The second configuration consisted of a hybrid system with Sm-TiO_2 adsorption and Z42/Z UF (in the same set-up). The feed tank was at first fed by a mixture of distilled water and Sm-TiO_2 at a concentration of 100 mg/L with a mild stirring, then the suspension was pumped from the feed tank to the membrane module. After circulation for 30 min, a dynamic layer was formed on the Z42/Z membrane surface. The tank was then emptied and the suspension was replaced by the dye solution to be treated. Permeate samples were collected for analysis as shown in Fig. 2. All experiments were performed at room temperature and a transmembrane pressure of 3 bar.

2.6. Determination of different fouling resistance abilities

The fouling resistance ability using the different configurations, UF alone; adsorption/UF and dynamic membrane were evaluated under a pressure of 3 bar. Two parameters namely flux recovery ratio (FRR) and flux decay ratio (FDR) could be calculated according to the following equations.

$$\text{FDR} = \frac{J_w - J_c}{J_w} \times 100 \tag{4}$$

$$\text{FRR} = \frac{J_{\text{wa}}}{J_w} \times 100 \tag{5}$$

where J_w is the water permeate flux of the clean membrane, J_c is the stabilized permeate flux of the membrane using the wastewater. J_{wa} is the water permeate flux of the membrane measured after a simple rinsing of the membrane with distilled water after treatment of wastewater.

3. Results and discussion

3.1. Adsorption study of indigo blue dye

3.1.1. Effect of adsorbent dose

It is well known that the quantity of adsorbent is an important factor that affects dye removal. In order to determine the optimal amount of Sm-TiO_2 (minimum amount) that shows maximum adsorption, the effect of the NC dose on IB removal was studied by preparing eight doses from 10 to 400 mg/L of NC and maintaining constant all other parameter conditions (100 mL of dye solutions, C_i = 25 mg/L, temperature = 25°C, pH = 2.5 and t = 240 min). It is evident from Fig. 3 that while the quantity of Sm-TiO_2 increases, the percentage (%) removal increases from 24.6% (at 10 mg/L) to 73.5% (at 100 mg/L). From a dose of 100 mg/L, the % of elimination of the IB does not change anymore. This result may be attributed to the high surface area and consequently, the availability of more unsaturated (active) adsorption sites, as already mentioned in previous studies [29–31]. Indeed, an excessive increase in adsorbent dose can create agglomeration of NC particles, resulting in a reduction in the total adsorption surface area and therefore a decrease in the quantity of dye molecules per unit mass of

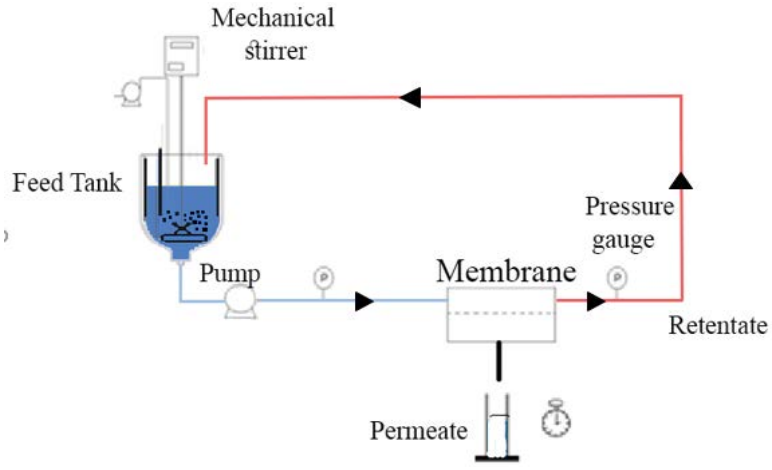

Fig. 2. Schematic representation of the hybrid adsorption-UF experimental set-up.

adsorbent. Consequently, a dose of 100 mg/L for Sm-TiO_2 was taken as the optimum in this work.

Previously, Mahzoura et al. [32] study the adsorption of IB by raw smectite. They demonstrated that 400 mg/L of smectite was the optimum dose which is much higher than the optimal dose achieved in the present work, demonstrating that the modified smectite (Sm-TiO_2) is more efficient for dyes removal than raw smectite.

3.1.2. Effect of contact time

Generally, the adsorption efficiency is strongly influenced by the contact time. In addition, this parameter is very important because it allows to save energy and to decrease the process cost on an industrial scale. To study the effect of this parameter on the adsorption of IB onto Sm-TiO_2, the reaction time was varied between 10 and 300 min. Fig. 4 shows that the % IB elimination increases instantaneously at the beginning of the experience to about 30% during the first 10 min and then continues to gradually increase with time until it reaches equilibrium within 240 min showing a maximum efficiency of IB retention of about 73.1%.

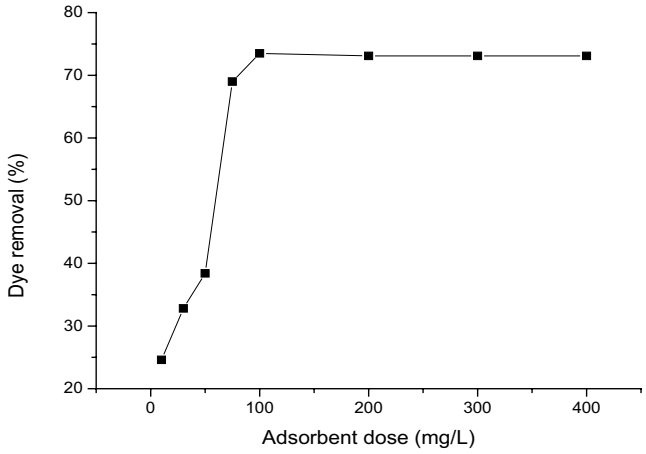

Fig. 3. Effect of adsorbent dosage of NC on IB dye removal (C_i = 25 mg/L; T = 25°C; pH = 2.5; t = 240 min).

Lopes et al. [33] obtained the equilibrium adsorption of food dye sunset yellow onto steam-activated carbon from malt bagasse within 240 min. The rapid kinetics observed at the start of the experience may be interpreted by the availability of numbers of active sites on the Sm-TiO_2 surface at the start of adsorption [34,35]. Shoukat et al. [36] interpreted the slow Crystal violet (CV) removal through the saturation of binding adsorption sites leading the CV ions to occupy the remaining vacant adsorption sites slowly owing to repulsive forces between the free CV ions and CV ions already adsorbed. According to El Ouardi et al. [37], the rapid kinetic corresponds to the external mass transfer while the slow kinetics is related to the internal mass transfer (diffusion phenomenon). It can be concluded that the best % adsorption of IB onto Sm-TiO_2 was achieved at t = 240 min. Thereafter this duration of the tests will be fixed in the rest of our work.

3.1.3. Effect of pH

As already mentioned by Saeed et al. [38], the ionization and dissociation of functional groups on the dye molecule (adsorbate) and the surface properties of the adsorbent are affected by the pH of an aqueous solution. For that, the study of this factor is necessary to know more about the adsorption process of IB molecules onto the Sm-TiO_2. The pH of the IB solution was adjusted between 1.5 and 9. Fig. 5 shows that the (%) elimination of IB is higher at acidic pH (from 1.5 to 3) and decreases rapidly from pH = 3. The (%) adsorption of IB becomes very slow at pH = 7, being 20%, and decreases to 5% at pH 9. Kumar and Kacha [39] found the same behavior by studying the adsorption of a basic dye on sawdust. They proposed that in case the solution becomes very basic, a competition probably happens between the Na^+ cations of NaOH, smaller and more mobile than those of the dye, thus stopping them from acceding to the surface of the adsorbent. This decrease can be explained also by the electrostatic interactions between Sm-TiO_2 and IB molecules. Indeed, the isoelectric pH (pH_i) of the Sm-TiO_2 is equal to 1.8 [40]. Therefore, the surface of the Sm-TiO_2 is positively charged when the pH is lower than pH_i, which favors the attraction between the anionic

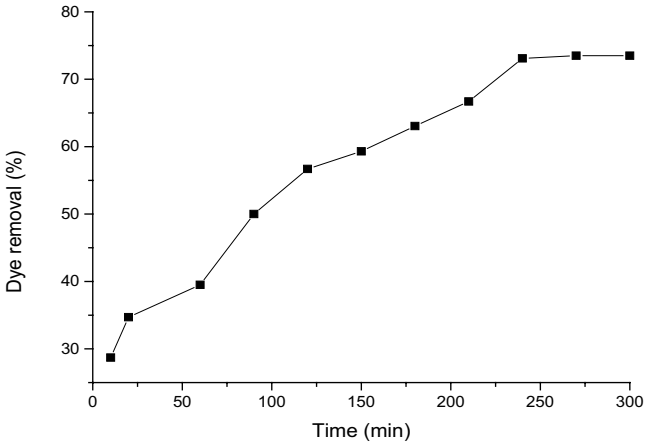

Fig. 4. Effect of the contact time on dye removal (C_i = 25 mg/L; D = 100 mg/L; T = 25°C; pH = 2.5).

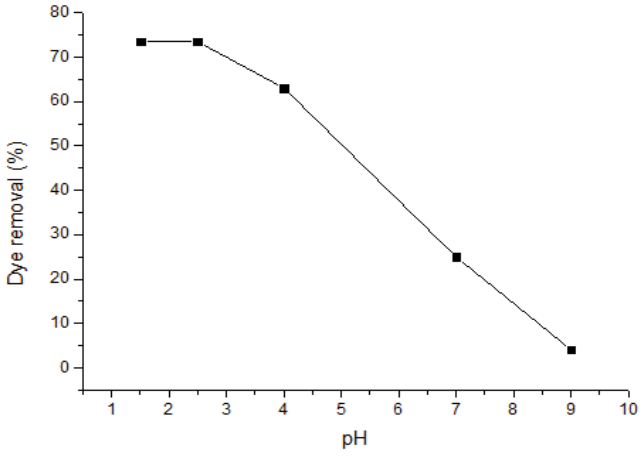

Fig. 5. Effect of pH on IB dye removal (C_i = 25 mg/L; D = 100 mg/L; T = 25°C; t = 240 min).

IB dye and the NC at acidic pH, and explains the high retention. Chaari et al. [41] compared the adsorption of the two dyes, one cationic and the other anionic, on nanoparticles (natural clay). Similar behavior was observed by Chaari et al. [41] considering the adsorption of anionic dyes by smectite-rich natural clays. It can be assumed that adsorption under the studied conditions is controlled by electrostatic interactions.

The highest removal yield takes place at pH = 2.5 which justifies the choice of this pH value for the next experiments.

On another way, the mechanism of adsorption depends primarily on functional behaviors but also on surface porosities of both adsorbent and adsorbate molecules. The IB dye molecules can be trapped on the adsorbent pore by electrostatic and hydrogen bonding interaction from free –NH and –C=O. The porous feature of Sm-TiO_2 can be then changed after adsorption.

3.1.4. Effect of initial IB concentration

The influence of initial IB concentration (5–40 mg/L) on the adsorption efficiency of Sm-TiO_2 was studied and the percentages of dye removal are given in Fig. 6. A slight decrease in IB removal for initial concentrations ranging from 5 to 20 mg/L was observed. Higher than these values, the increase of initial concentration to 40 mg/L leads to a decrease in performance from 92.5% (at 20 mg/L) to 65% (at 40 mg/L). Similar behavior was observed by Cherifi et al. [43], where a decrease in the removal of MB by NC from 98% at 40 mg/L to 43% at 120 mg/L was obtained. At low concentrations, the ratio between active sites of Sm-TiO_2 and IB molecules is very important and all molecules can be retained. Based on these results, the concentration C_i = 20 mg/L was considered as an optimal concentration allowing the maximum removal of IB of about 92.5%. This means that for any IB solution with a concentration below this value, almost all of the IB molecules are retained by the Sm-TiO_2. Unlike the % of adsorbed dye, the adsorption capacity (q) of Sm-TiO_2 increased from 48.5 mg/g (at 5 mg/L) to 260.04 mg/g (at 40 mg/L). A similar phenomenon has been demonstrated by other researchers [36]. In fact, the increase in concentration induces an increase in the driving force of the concentration gradient, thus increasing the diffusion of the dye molecules in solution through the surface of the adsorbent [42].

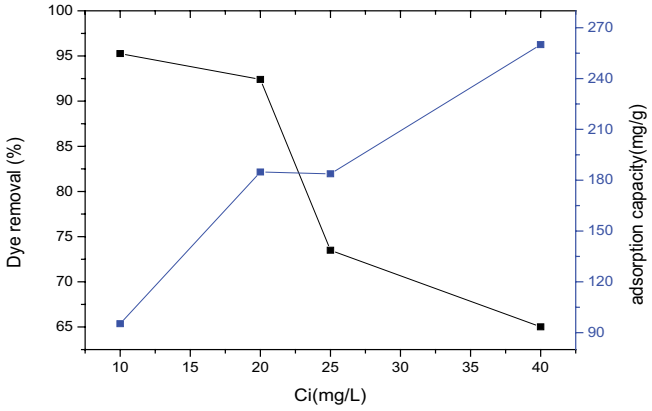

Fig. 6. Effect of initial IB concentration on dye removal (D = 100 mg/L; pH = 2.5; t = 240 min; T = 25°C).

The adsorption capacity of Sm-TiO_2 for the IB dye was compared to other adsorbents as presented in Table 2, indicating that Sm-TiO_2 NC showed promising adsorption efficiencies for anionic dyes.

3.1.5. Adsorption kinetics

Kinetic models are often used to correlate empirical adsorption data in order to understand the mechanisms of the adsorption process. The most commonly kinetic models used are [47]: the pseudo-first-order model and the pseudo-second-order model. The linearized form of the pseudo-first-order rate equation (by Lagergren) is given as:

$$\ln\left(q_e - q_t\right) = \ln q_e - k_1 t \tag{6}$$

where q_t and q_e are the amounts of IB molecules adsorbed at t (min) and equilibrium (mg/g), respectively, and k_1 is the rate constant (min^{-1}). The adsorption rate constants k_1 can be obtained experimentally from the plot of Ln(q_e − q_t) vs. t (Fig. 7). Kinetics models have been also determined by the pseudo-second-order with the linearized equation:

$$\frac{t}{q_t} = \frac{1}{\left(k_2 q_e^2\right)} + \frac{t}{q_e} \tag{7}$$

Table 2
Comparison of adsorption capacities of Sm-TiO_2 with various adsorbents in presence of dye solution

Adsorbent	Dye	q_e (mg/g)	References
Activated carbon	Indigo blue	53	[32]
Smectite (natural clay)		57	
Activated carbon	Acid green 1	24	[44]
Natural clay	Crystal violet	25.9	[45]
Na^+_exchanged clay (EP-Na)	Crystal violet	99.84	[46]
	Methyl orange	26.85	
Hexadecylpyridinium ($HDPy^+$)_modified clay (EP-HDPy3CEC)	Crystal violet	53.87	[46]
	Methyl orange	99.32	
Sm-TiO_2	Indigo blue	183.75	This study

where k_2 (g/mg min) is the rate constant of adsorption and q_e is the equilibrium adsorption capacity (mg/g). Both parameters are calculated from the plot of t/q_t vs. t (Fig. 8).

The results summarized in Table 3, show that the two kinetics models correlate well with the experimental values (R = 0.97 for the first-order model and R = 0.94 for the pseudo-second-order model). However, the adsorption capacity (q_e) obtained from the pseudo-second-order model is closer to that found experimentally (q_{exp} = 183.75 mg/g). Therefore, the pseudo-second-order model is best adapted to describe the adsorption kinetics in our case. When active sites on the Sm-TiO_2 surface have come to saturation, IB molecules begin to enter the adsorbed pores and adsorbed onto the inner walls. The low k_2 value confirms the sluggish diffusion of IB through the pores. This result was confirmed by Mahzoura et al. [32] who found that in the presence of three different types of adsorbents, natural clay, natural zeolite, and activated carbon, adsorption kinetics followed the pseudo-second-order models.

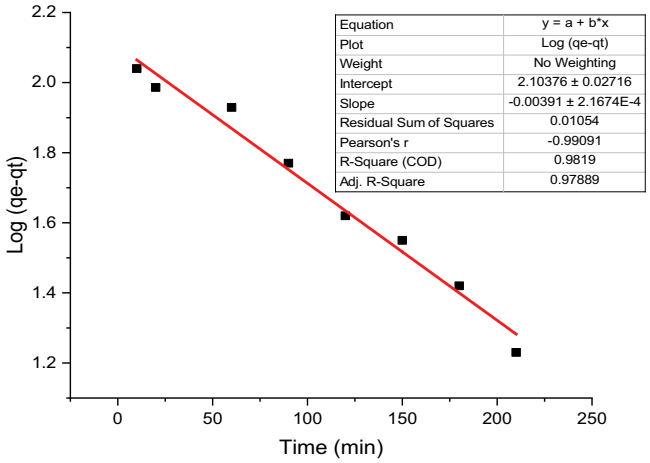

Fig. 7. Correlation of adsorption data of IB on Sm-TiO_2 by a pseudo-first-order equation.

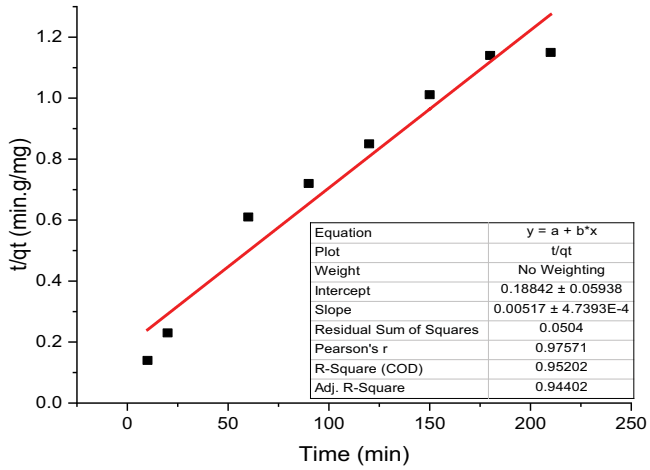

Fig. 8. Correlation of adsorption data of IB on Sm-TiO_2 by a pseudo-second-order.

3.1.6. Adsorption isotherms

The study of adsorption isotherms is essential to identify how IB molecules interact with the Sm-TiO_2 surface. The modeling of equilibrium adsorption consists in representing, by mathematical laws, the relationship between the quantity of dye molecules in the liquid phase (C_e) and that adsorbed on the NC (q_e), at equilibrium. For that, two isotherm models, the Langmuir [48] and Freundlich [49] models were applied to analyze the obtained experimental results. The Langmuir adsorption model assumes that all active sites on the adsorbent surface are similar, there is no interaction between adsorbed molecules and the adsorbent surface is coated with a monolayer. The results of the IB dye adsorption tests on Sm-TiO_2 were analyzed with the Langmuir model represented by Eq. (8):

$$\frac{C_e}{q_e} = \frac{1}{q_{max} \cdot K_L} + \frac{C_e}{q_{max}} \tag{8}$$

On the basis of a dimensionless equilibrium parameter R_L [50] a more thorough examination of the Langmuir equation can be carried out, also known as the separation factor, which is calculated as follows:

$$R_L = \frac{1}{\left(1 + K_L\left(C_0\right)\right)} \tag{9}$$

The value of R_L lies between 0 and 1 for favorable adsorption, while $R_L > 1$ represents unfavorable adsorption, and $R_L = 1$ represents linear adsorption while the adsorption process is irreversible if $R_L = 0$.

q_e is the equilibrium amount of IB molecules adsorbed onto the Sm-TiO_2 (mg/g), C_e is the IB concentration in the solution (mg/L) at equilibrium, q max is the monolayer adsorption capacity of the adsorbent (mg/g), R_L is the separation factor, C_0 is the IB initial concentration (mg/L) and K_L is the Langmuir adsorption constant (L/mg). The parameters q_{max} and K_L are determined from the slope and intersection with the y-axis of the correlation of C_e/q_e vs. C_e (Fig. 9).

The Freundlich isotherm assumes that adsorption is multilayer and the adsorbent surface is heterogeneous. It can be expressed by the following relationship:

Table 3
Calculated kinetic parameters for the pseudo-first-order and pseudo-second-order models for IB dye removal by Sm-TiO_2

Adsorbent	Pseudo-first-order			Pseudo-second-order		
Sm-TiO_2 (q_{exp} = 183.75 mg/g)	k_1 (min^{-1})	q_e (mg/g)	R^2	k_2 (g/mg min)	q_e (mg/g)	R^2
	0.0099	135.83	0.97	0.00015	188.67	0.94

$$\ln q_e = \ln K_F + \frac{1}{n}\ln C_e \quad (10)$$

where K_F is an empirical constant (mg/g) indicating the adsorption capacity and $1/n$ is an empirical parameter, indicating the adsorption intensity. K_F and $1/n$ are obtained from the slope and intercept of the correlation of $\log q_e$ vs. $\log C_e$ (Fig. 10).

The estimated adsorption constants for the two models are listed in Table 4. As observed, the correlation factor (R^2 = 0.94) of the Langmuir model is higher than that of the Freundlich model (R^2 = 0.77). The dimensionless parameter R_L stays between 0 and 1 (R_L = 0.26), indicating that a favorable adsorption procedure is required. Therefore, the adsorption of IB dye on Sm-TiO_2 follows the Langmuir model better than the Freundlich model, suggesting that Sm-TiO_2 are covered by a monolayer of IB molecules without any interaction between them.

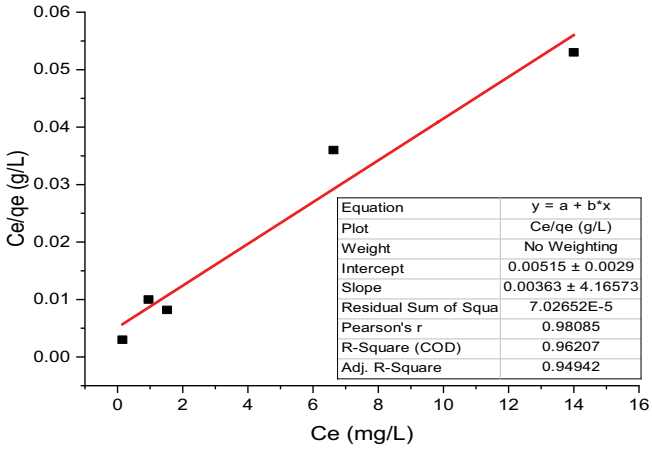

Fig. 9. Adsorption isotherm of IB onto Sm-TiO_2, correlation with the Langmuir model.

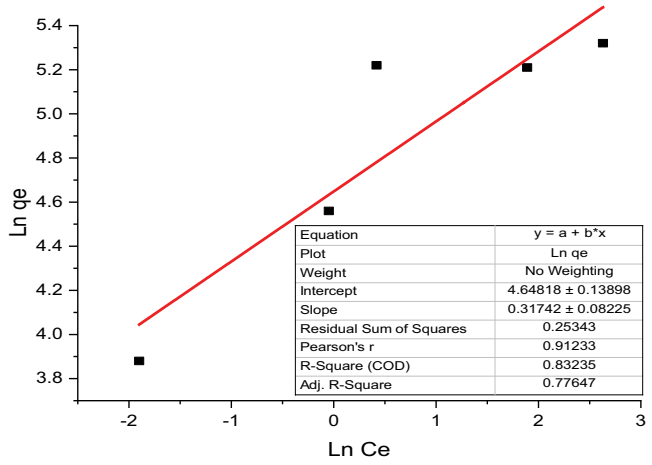

Fig. 10. Adsorption isotherm of IB onto Sm-TiO_2, correlation with the Freundlich model.

Table 4
Adsorption isotherm constants for adsorption of IB onto Sm-TiO_2

Langmuir isotherm parameters				Freundlich isotherm parameters		
K_L (L/mg)	q_{max} (mg/g)	R_L	R^2	K_F (mg/g) $(L/mg)^{1/n}$	$1/n$	R^2
0.0707	333.33	0.26	0.96	15.18	0.14	0.77

3.1.7. Adsorption thermodynamics

The study of adsorption thermodynamics is essential as it plays an important role in the processes of adsorption [51]. The thermodynamic parameters, such as free energy ($\Delta G°$), enthalpy variation ($\Delta H°$) and entropy variation ($\Delta S°$), show the feasibility and spontaneous nature of the adsorption phenomenon. These parameters are given by Eqs. (11) and (12) (Van't Hoff equation) [52]:

$$\Delta G° = -RT\ln K_d \quad (11)$$

$$\ln K_d = \frac{\Delta S°}{R} - \frac{\Delta H°}{RT} \quad (12)$$

where $\Delta G°$ is the standard free energy change, R is the universal gas constant 8.314 (J/mol K), T is the absolute temperature (K), K_d is the equilibrium constant, $\Delta H°$ and $\Delta S°$ are the enthalpy and entropy of sorption reaction, respectively. These parameters are estimated from equilibrium adsorption isotherms at different temperatures (from 293 to 323 K) (Fig. 11) by using a thermostatic bath to keep the temperature at the desired value.

As shown in Table 5, the values of $\Delta S°$ and $\Delta H°$ are negative, this result implies that adsorption of IB molecules on Sm-TiO_2 is exothermic and spontaneous and that it does not gain energy from external resources [53,54]. In addition, the negative value of $\Delta H°$ below 40 kJ/mol suggests that in this case, the adsorption is a physical process (physisorption) [55]. Therefore, we can deduce that the interactions between the Sm-TiO_2 and the IB molecules are ensured by

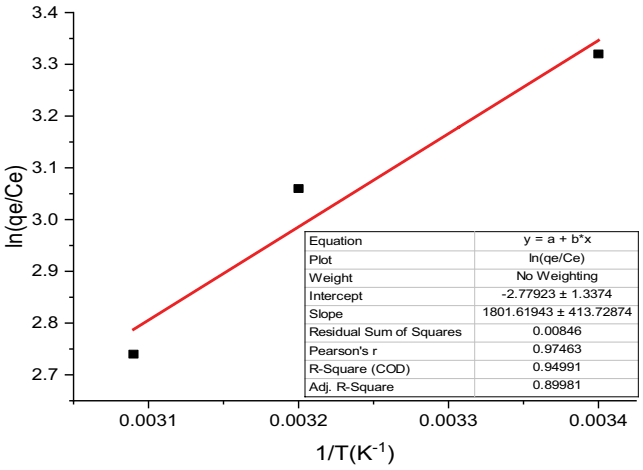

Fig. 11. The plot of $\ln K_d$ vs. $1/T$ for estimation of thermodynamic parameters that govern the adsorption of IB onto Sm-TiO_2.

electrostatic forces such as dipoles, hydrogen or van der Waals bonds and the process takes place by forming multilayers of IB dye molecules that can be adsorbed to the surface of the material, this phenomenon being rapid and reversible. In the temperature range of 298–323°C, $\Delta G°$ values are less negative when the temperature increases, indicating that the adsorption process is thermodynamically achievable at room temperature. This observation also confirms that the adsorption phenomenon is exothermic. In addition, $\Delta G°$ is between –8.23 and –7.52 kJ/mol suggesting that adsorption is dominated by low-energy attraction forces [56].

3.1.8. Fourier-transform infrared spectroscopy study

Fig. 12 shows the FTIR analysis of Sm-TiO_2 adsorbent before (a) and after (b) adsorption of IB dye. The new peaks that appeared in the FTIR spectrum after adsorption of IB dye (b) confirmed the success of the adsorption phenomenon on the surface of Sm-TiO_2. One notices the appearance of peaks at 1,625 cm^{-1} assigned to the carbonyl groups (C=O), evidencing the presence of the IB dye on the Sm-TiO_2 surface [35]. In addition, the peaks between 1,584 and 1,316 cm^{-1} are attributed to C=C aromatic stretching [35].

3.2. Performances of adsorption/UF hybrid process

3.2.1. Performances of the Z42/Z membrane

The objective of this part of the study was to evaluate the efficiency of the UF zeolite membrane Z42/Z for the removal of IB molecules from a synthetic solution. Fig. 13 shows the variation of the permeate flux for UF alone as a function of time at room temperature, applying a transmembrane pressure ΔP = 3 bar, and using a synthetic IB solution with pH = 2.5 and C_i = 25 mg/L. During the first 20 min, the permeate flux gradually decreased from 111 to 71.5 L/m^2 h. This decrease may be due to the adsorption of IB molecules from the solution, inducing a polarization concentration layer and a pore-clogging phenomenon, as well as an increase of the solution viscosity [57].

However, the first configuration (hybrid), where the IB dye is treated by adsorption onto Sm-TiO_2 (adsorption was used as pretreatment step) before filtrating by UF zeolite, is more efficient for the permeate flux. We observed that the UF process was enhanced by the adsorption technique. The stabilized flux increased from 71 L/h m^2 for UF alone to 226 L/h m^2 for the hybrid process. So, the pretreatment by Sm-TiO_2 succeeded to enhance UF performance in terms of permeate flux and limitation of membrane fouling.

In addition, the IB dye retentions were high, both for a simple UF and a hybrid treatment with Sm-TiO_2 NCs. In both cases, the dye retentions stabilized at 97.7%. This result confirmed the efficacy of the Z42/Z membrane.

Table 5
Thermodynamic adsorption parameters of IB onto Sm-TiO_2

	$\Delta G°$ (kJ/mol)			$\Delta H°$ (kJ/mol)	$\Delta S°$ (J/mol K)
T (K)	298	313	323		
Sm-TiO_2	–8.23	–7.79	–7.52	–16.62	–28.19

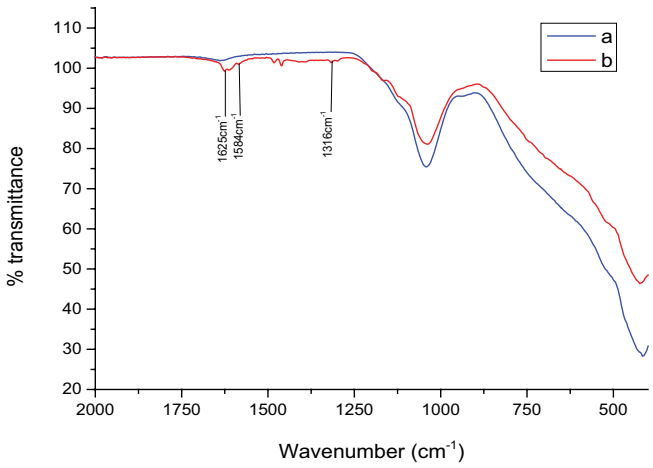

Fig. 12. FTIR spectra of Sm-TiO_2 (a) before IB adsorption and (b) after IB adsorption.

3.2.2. UF-adsorption hybrid system (dynamic layer)

The tests were carried out at different pH levels, Sm-TiO_2 doses and initial IB concentrations. Using acidic (HCl 0.1 M) or basic (NaOH 0.1 M) solutions, the feed pH was modified in the range of 2–8.5. In the feed tank, the adsorbent dose was adjusted to be between 50 and 200 mg/L. The initial dye concentration was varied to be between 12.5 and 50 mg/L. Every 5 min, the permeate flux was determined.

3.2.2.1. Effect of pH

According to Fig. 14, pH had a clear effect on the hybrid process behavior in terms of permeate flux. The stabilized permeate flux decreased when pH increased. It was 182 L/h m^2 for pH 2 and it decreased to 125 L/h m^2 at pH 8.5. The higher permeate flux was obtained at the acidic solution, 182 and 179 L/h m^2, for pH equals to 2 and 4, respectively. This result can be explained by the intensity of the electric attraction or repulsion between the IB molecules and the dynamic membrane. The dynamic membrane was

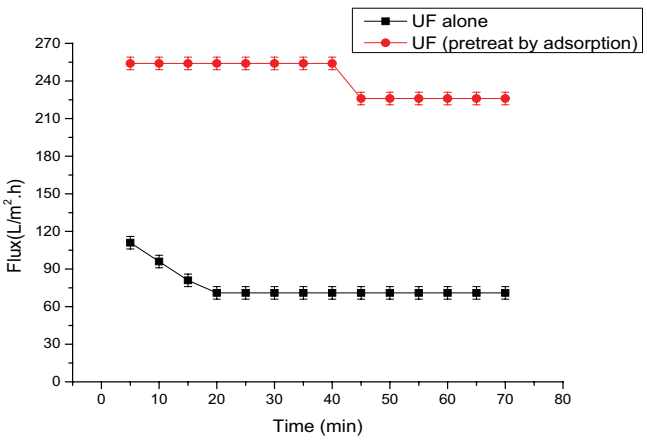

Fig. 13. Permeate flux in UF alone and hybrid process (T = 25°C; TMP = 3 bar).

formed by a dynamic layer based on Sm-TiO_2 when the pHpzc (the point of zero charges) of these NCs is 1.8 [28]. Therefore, the dynamic membrane is negatively charged for a pH > 1.8 and positively charged for a pH < 1.8. The dynamic membrane played two roles, UF and adsorption in one unit, for a pH below or near to1.8. This result was previously shown by Aloulou et al. [28], as heavy metal retention efficiency was predominantly affected by pH, with the highest rejection rate occurring near pHpzc.

The adsorption of IB molecules decreased when pH increased, as the dynamic membrane loses its second function (adsorption role) which explains the decrease in stabilized permeate flux.

The permeate fluxes were very close for pH values of 2 and 4 (182 and 179 L/m² h). As it is more favorable to work at less acidic pH, the value of 4 was selected as an optimum pH.

3.2.2.2. *Effect of Sm-TiO_2 dose*

According to Fig. 15, in the case of a hybrid system, the filtration flux remained constant regardless of the added dose. The stabilization of the flux over time indicates that the addition of adsorbent avoids membrane fouling. Hammami et al. [26] used PAC in the PAC/UF hybrid system to remove Acid orange 7 (AO7). They noticed that the permeate flux was stabilized for different PAC doses (between 50 and 300 mg/L). This behavior can be explained by the role of the dynamic layer of Sm-TiO_2 in inhibiting the clogging of the UF membrane by capturing the dye molecules in the thickness of the deposit [58]. Indeed, once formed, the nanoparticle layer reduces the pore size of the UF membrane and then forms a dynamic UF membrane.

Fig. 15 shows that the permeate flux decreased from 182 L/m² h for an added dose of 50 to 160 L/m² h for 200 mg/L. The Sm-TiO_2 doses equal to 50 and 100 mg/L were sufficient to adsorb enough IB molecules, consequently, the membrane Z42/2 fouling was reduced and the permeate flux was enhanced. The optimal dose of adsorbent in the hybrid process was 50 mg/L. This dose was reduced compared to the optimal dose in the case of adsorption alone (100 mg/L).

The permeate flux decreased slightly when Sm-TiO_2 was added in excess of 100 mg/L. This result was anticipated because raising the Sm-TiO_2 dose, led to an increase in the thickness of the dynamic layer and therefore a higher resistance to the permeation.

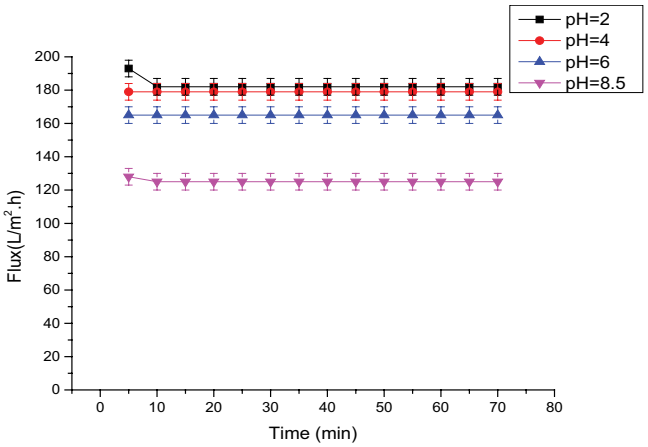

Fig. 14. Effect of pH on permeate flux (C_i = 25 mg/L; D = 100 mg/L; TMP = 3 bar).

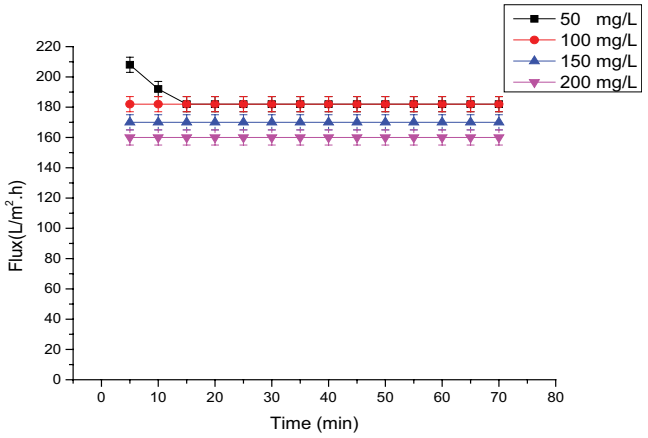

Fig. 15. Effect of Sm-TiO_2 dose on permeate flux (C_i = 25 mg/L; pH = 4; TMP = 3 bar).

3.2.2.3. *Effect of IB concentrations*

Fig. 16 shows the effect of IB dye concentration on the permeate flux of the dynamic membrane (hybrid process). When the IB concentration was increased from 12.5 to 50 mg/L, the stabilized permeate flux decreased steadily (from 196 to 170 L/m² h). This result was expected because the effectiveness of the membrane depends on the initial quality of the effluent to be treated. The flux decreases due to increased resistance in the more concentrated solution near the membrane surface. An increase in IB dye concentration can cause blocked pores, as a result, the flow encounters more resistance [25].

Indeed, a high permeate quality value can be maintained during treatment with the hybrid process. The IB dye retention at all conditions was higher than 97%. It seems that the Z42/Z UF membrane represents an efficient solution

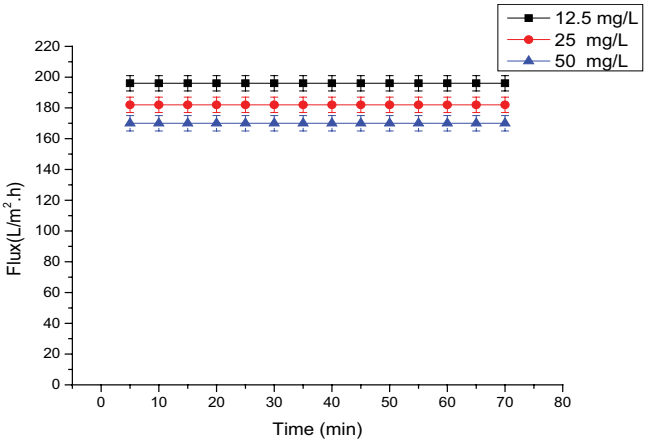

Fig. 16. Effect of initial IB concentration on permeate flux (pH = 4; D = 50 mg/L; TMP = 3 bar).

Table 6
Determination of the flux decay ratio and the flux recovery ratio for different membrane process

	J_w (L/h m^2)	J_c (L/h m^2)	J_{wa} (L/h m^2)	FDR (%)	FRR (%)
UF alone	348	71.5	222	79.45	63.79
Adsorption/UF	348	226	320	35.05	91.95
Dynamic membrane	270	179	250	33.7	92.59

for dye removal. The obtained quality of the treated water means that it can be reused or recycled. Moreover, the usage of a dynamic membrane reduced reaction time and reduced Sm-TiO_2 dose.

3.3. Fouling resistance ability

During the ultrafiltration process, the fouling is coupled with an evident deterioration of the membrane surface. To determine the fouling resistance ability during the different considered approaches, UF alone; adsorption/UF and dynamic membrane, the following parameters, the FRR and the FDR were calculated and illustrated in Table 6.

FRR values show the percentage recovery of the original water permeability of the membrane after utilization and rinsing with water. In fact, higher FRR values are more beneficial and prove better antifouling property. Moreover, FDR values indicate the percentage of the flux decays during the filtration process, so lower FDR values are more favorable [59].

From Table 6, it is clear that the dynamic membrane presents a higher FRR value (92.59%) and the less FDR value (33.7%). In addition, the adsorption pretreatment before UF allows the increase of the FRR from 63.79% to 91.95% and the decrease of FDR from 79.45% to 35.05%.

4. Conclusion

The current work reveals that Sm-TiO_2 NCs can be employed as an efficient adsorbent to remove IB dye from aqueous solutions. The adsorption capacity of dye uptake (mg/g) was observed to rise as Sm-TiO_2 dose, contact time and initial dye concentration increased up to well-determined values. The efficiencies of Sm-TiO_2 NCs decreased as the pH values increased. The success of the adsorption process of IB dye onto Sm-TiO_2 was confirmed by a higher equilibrium capacity adsorption above 180 mg/g with IB dye removal beyond 70%. The Langmuir isotherm equation suited the equilibrium data better than that of Freundlich. The dimensionless separation factor (R_L) showed that Sm-TiO_2 could be applied for IB dye removal from aqueous solutions. The modeling of the adsorption kinetics was confirmed by the pseudo-second-order model with a good correlation. Thermodynamic parameters such as $\Delta G°$, $\Delta H°$ and $\Delta S°$ showed that the adsorption was spontaneous and exothermic.

Two configurations for the hybrid process were applied. In the first configuration, the adsorption by Sm-TiO_2 was used as a pretreatment step before UF. In the second configuration, adsorption and UF separation were integrated into one unit (dynamic membrane). The results indicated that for the two configurations the permeate flux remained almost stable while a higher decrease was observed when UF alone was applied. The application of the dynamic membrane caused a reduction in reaction time and Sm-TiO_2 dose, the highest permeate was obtained for a pH equal to 4 and a Sm-TiO_2 dose of 50 mg/L.

Acknowledgments

This work was financially supported by the PHC-UTIQUE program N° 20G1205.

References

[1] P. Lene, M. Heynen, F. Pellicciotti, Freshwater Resources: Past, Present, Future, in: International Encyclopedia of Geography: People, the Earth, Environment and Technology, Wiley, 2019, doi: 10.1002/9781118786352.
[2] C.O. Panão, E.L.S. Campos, H.H.C. Lima, A.W. Rinaldi, M.K. Lima-Tenório, E.T. Tenório-Neto, M.R. Guilherme, T. Asefa, A.F. Rubira, Ultra-absorbent hybrid hydrogel based on alginate and SiO_2 microspheres: a high-water-content system for removal of methylene blue, J. Mol. Liq., 276 (2019) 204–213.
[3] K.C. Bedin, I.P.A.F. Souza, A.L. Cazetta, L. Spessato, A. Ronix, V.C. Almeida, CO_2-spherical activated carbon as a new adsorbent for methylene blue removal: kinetic, equilibrium and thermodynamic studies, J. Mol. Liq., 269 (2018) 132–139.
[4] Z. Duan, Y. Li, M. Zhang, H. Bian, Y. Wang, L. Zhu, D. Xia, Towards cleaner wastewater treatment for special removal of cationic organic dye pollutants: a case study on application of supramolecular inclusion technology with β-cyclodextrin derivatives, J. Cleaner Prod., 256 (2020) 120308, doi: 10.1016/j.jclepro.2020.120308.
[5] M. Bilal, M. Asgher, M. Iqbal, H. Hu, X. Zhang, Chitosan beads immobilized manganese peroxidase catalytic potential for detoxification and decolorization of textile effluent, Int. J. Biol. Macromol., 89 (2016) 181–189.
[6] C.P. Ukpaka, E. Wami, S. Amadi, Effect of pollution on metal corrosion: a case study of carbon steel metal in acidic media, Curr. Sci. Perspect., 1 (2015) 107–111.
[7] J. Mittal, Permissible synthetic food dyes in India, Reson. – J. Sci. Educ., 25 (2020) 567–577.
[8] Z. Huang, Y. Li, W. Chen, J. Shi, N. Zhang, X. Wang, Z. Li, L. Gao, Y. Zhang, Modified bentonite adsorption of organic pollutants of dye wastewater, Mater. Chem. Phys., 202 (2017) 266–276.
[9] I. Ali, C. Peng, I. Naz, D. Lin, D.P. Saroj, M. Ali, Development and application of novel bio-magnetic membrane capsules for the removal of the cationic dye malachite green in wastewater treatment, RSC Adv., 9 (2019) 3625–3646.
[10] J. Joseph, R.C. Radhakrishnan, J.K. Johnson, S.P. Joy, J. Thomas, Ion-exchange mediated removal of cationic dye-stuffs from water using ammonium phosphomolybdate, Mater. Chem. Phys., 242 (2020) 122488, doi: 10.1016/j.matchemphys.2019.122488.
[11] M. Benjelloun, Y. Miyah, G.A. Evrendilek, F. Zerrouq, S. Lairini, Recent advances in adsorption kinetic models: their application to dye types, Arabian J. Chem., (2021) 103031, doi: 10.1016/j.arabjc.2021.103031.
[12] H. Aloulou, A. Ghorbel, W. Aloulou, R. Ben Amar, S. Khemakhem, Removal of fluoride ions (F−) from aqueous solutions using modified Turkish zeolite with quaternary ammonium, Environ. Technol., 42 (2021) 1353–1365.
[13] A. Kausar, M. Iqbal, A. Javed, K. Aftab, Zill-i-Huma Nazli, H.N. Bhatti, S. Nouren, Dyes adsorption using clay and modified clay: a review, J. Mol. Liq., 256 (2018) 395–407.
[14] A. Mittal, R. Ahmad, I. Hasan, Iron oxide-impregnated dextrin nanocomposite: synthesis and its application for the biosorption of Cr(VI) ions from aqueous solution, Desal. Water Treat., 57 (2015) 15133–15145.

[15] A. Mariyam, J. Mittal, F. Sakina, R.T. Baker, A.K. Sharma, A. Mittal, Efficient batch and fixed-bed sequestration of a basic dye using a novel variant of ordered mesoporous carbon as adsorbent, Arabian J. Chem., 14 (2021) 103186, doi: 10.1016/j.arabjc.2021.103186.
[16] M.B. Chabalala, M.Z. Al-Abri, B.B. Mamba, E.N. Nxumalo, Mechanistic aspects for the enhanced adsorption of bromophenol blue and atrazine over cyclodextrin modified polyacrylonitrile nanofiber membranes, Chem. Eng. Res. Des., 169 (2021) 19–32.
[17] E. Daneshvar, A. Vazirzadeh, A. Niazi, M. Kousha, Mu. Naushad, A. Bhatnagar, Desorption of methylene blue dye from brown macroalga: effects of operating parameters, isotherm study and kinetic modeling, J. Cleaner Prod., 152 (2017) 443–453.
[18] J. Chang, J. Ma, Q. Ma, D. Zhang, N. Qiao, M. Hu, H. Ma, Adsorption of methylene blue onto Fe_3O_4/activated montmorillonite nanocomposite, Appl. Clay Sci., 119 (2016) 132–140.
[19] R. Msaadi, A. Gharsalli, S. Mahouche-Chergui, S. Nowak, H. Salmi, B. Carbonnier, S. Ammar, M.M. Chehimi, Reactive and functional clay through UV-triggered thiol-ene interfacial click reaction, Surf. Interface Anal., 48 (2016) 532–537.
[20] J. Mittal, Recent progress in the synthesis of Layered Double Hydroxides and their application for the adsorptive removal of dyes: a review, J. Environ. Manage., 295 (2021) 113017, doi: 10.1016/j.jenvman.2021.113017.
[21] H. Liu, Y. Sun, T. Yu, J. Zhang, X. Zhang, H. Zhang, K. Zhao, J. Wei, Plant-mediated biosynthesis of iron nanoparticles-calcium alginate hydrogel membrane and its eminent performance in removal of Cr(VI), Chem. Eng. J., 378 (2019) 122120, doi: 10.1016/j.cej.2019.122120
[22] J. Tang, H. Jia, S. Mu, F. Gao, Q. Qin, J. Wang, Characterizing synergistic effect of coagulant aid and membrane fouling during coagulation–ultrafiltration via in-situ Raman spectroscopy and electrochemical impedance spectroscopy, Water Res., 172 (2020) 115477, doi: 10.1016/j.watres.2020.115477.
[23] P. Bhattacharya, S. Ghosh, A. Mukhopadhyay, Efficiency of combined ceramic microfiltration and biosorbent based treatment of high organic loading composite wastewater: an approach for agricultural reuse, J. Environ. Chem. Eng., 1 (2013) 38–49, doi: 10.1016/j.jece.2013.03.002.
[24] K.-Y. Kim, H.-S. Kim, J. Kim, J.-W. Nam, J.-M. Kim, S. Son, A hybrid microfiltration–granular activated carbon system for water purification and wastewater reclamation/reuse, Desalination, 243 (2009) 132–144.
[25] S.M. Alardhi, M.A. Talib, M.A. Jamal, A hybrid adsorption membrane process for removal of dye from synthetic and actual wastewater, Chem. Eng. Process., 157 (2020) 108113, doi: 10.1016/j.cep.2020.108113.
[26] A. Hammami, C. Charcosset, R. Ben Amar, Performances of continuous adsorption–ultrafiltration hybrid process for AO7 dye removal from aqueous solution and real textile wastewater treatment, J. Membr. Sci. Technol., 7 (2017), doi: 10.4172/2155-9589.1000171.
[27] W. Aloulou, W. Hamza, H. Aloulou, A. Oun, S. Khemakhem, A. Jada, S. Chakraborty, S. Curcio, R. Ben Amar, Developing of titania-smectite nanocomposites UF membrane over zeolite based ceramic support, Appl. Clay Sci., 155 (2018) 20–29.
[28] H. Aloulou, H. Bouhamed, M.O. Daramola, S. Khemakhem, R. Ben Amar, Fabrication of asymmetric ultrafiltration membranes from natural zeolite and their application in industrial wastewater treatment, Euro-Mediterr. J. Environ. Integr., 5 (2020) 1–11, doi: 10.1007/s41207-020-0150-9.
[29] A. Fegousse, Y. Miyah, R. Elmountassir, A. Lahrichi, Valorization of pineapple bark for removal of a cationic dye sush as methylene blue, J. Mater. Environ. Sci., 9 (2018) 2449–2457.
[30] A. Fegousse, Y.Miyah, R. Elmountassir, A. Lahrichi, Etude cinétique et thermodynamique de l'adsorption de bleu de méthylène sur les cendres de bois (Kinetic and thermodynamic study of the adsorption of methylene blue on wood ashes), J. Mater. Environ. Sci., 6 (2015) 3295–3306.
[31] A.H. Jawad, A.S. Abdulhameed, Mesoporous Iraqi red kaolin clay as an efficient adsorbent for methylene blue dye: adsorption kinetic, isotherm and mechanism study, Surf. Interfaces, 18 (2020) 100422, doi: 10.1016/j.surfin.2019.100422.
[32] M. Mahzoura, N. Tahri, M. Daramola, J. Duplay, G. Schäfer, R. Ben Amar, Comparative investigation of indigo blue dye removal efficiency of activated carbon and natural clay in adsorption/ultrafiltration system, Desal. Water Treat., (2019) 24361, doi: 10.5004/dwt.2019.24361.
[33] G.K.P. Lopes, H.G. Zanella, L. Spessato, A. Ronix, P. Viero, J.M. Fonseca, J.T.C. Yokoyama, A.L. Cazetta, V.C. Almeida, Steam-activated carbon from malt bagasse: optimization of preparation conditions and adsorption studies of sunset yellow food dye, Arabian J. Chem., 14 (2021) 103001, doi: 10.1016/j.arabjc.2021.103001.
[34] A.R. Dinçer, Y. Güneş, N. Karakaya, E. Güneş, Comparison of activated carbon and bottom ash for removal of reactive dye from aqueous solution, Bioresour. Technol., 98 (2007) 834–839.
[35] A. Rais, Studies on adsorption of Crystal violet dye from aqueous solution onto coniferous pinus bark powder (CPBP), J. Hazard. Mater., 171 (2009) 767–773.
[36] S. Shoukat, H.N. Bhatti, M. Iqbal, S. Noreen, Mango stone biocomposite preparation and application for Crystal violet adsorption: a mechanistic study, Microporous Mesoporous Mater., 239 (2017) 180–189.
[37] M. El Ouardi, S. Alahiane, S. Qourzal, A. Abaamrane, A. Assabbane, J. Douch, Removal of carbaryl pesticide from aqueous solution by adsorption on local clay in Agadir, Am. J. Anal. Chem., 4 (2013) 72–79.
[38] A. Saeed, S. Mehwish, I. Muhammad, Application potential of grapefruit peel as dye sorbent: kinetics, equilibrium and mechanism of Crystal violet adsorption, J. Hazard. Mater., 179 (2010) 564–572.
[39] B. Kumar, S. Kacha, Étude cinétique et thermodynamique de l'adsorption d'un colorant basique sur la sciure de bois, Revue des sciences de l'eau/J. Water Sci., 24 (2011) 131–144.
[40] W. Aloulou, H. Aloulou, M. Khemakhem, J. Duplay, M.O. Daramola, R. Ben Amar, Synthesis and characterization of clay-based ultrafiltration membranes supported on natural zeolite for removal of heavy metals from wastewater, Environ. Technol. Innovation, 18 (2020) 100794, doi: 10.1016/j.eti.2020.100794.
[41] I. Chaari, E. Fakhfakh, M. Medhioub, F. Jamoussi, Comparative study on adsorption of cationic and anionic dyes by smectite rich natural clays, J. Mol. Struct., 1179 (2019) 672–677.
[42] Z. Cherifi, B. Boukoussa, A. Mokhtar, M. Hachemaoui, F.Z. Zeggai, A. Zaoui, K. Bachari, R. Meghabar, Preparation of new nanocomposite poly(GDMA)/mesoporous silica and its adsorption behavior towards cationic dye, React. Funct. Polym., 153 (2020) 104611, doi: 10.1016/j.reactfunctpolym.2020.104611.
[43] F. Deniz, D. Saadet Saygideger, Investigation of adsorption characteristics of Basic Red 46 onto gypsum: equilibrium, kinetic and thermodynamic studies, Desalination, 262 (2010) 161–165.
[44] E. Mourid, M. Lakraimi, E. El Khattabi, L. Benaziz, M. Berraho, Removal of textile dye Acid green 1 from wastewater by activated carbon, J. Mater. Environ. Sci., 8 (2017) 3121–3130.
[45] Y. Miyah, A. Lahrichi, M. Idrissi, Kh. Anis, R. Kachkoul, N. Idrissi, S. Lairini, V. Nenov, F. Zerrouq, Removal of cationic dye "Crystal violet" in aqueous solution by the local clay, J. Mater. Environ. Sci., 8 (2017) 3570–3582.
[46] S. Gamoudi, E. Srasra, Removal of cationic and anionic dyes using purified and surfactant-modified Tunisian clays: kinetic, isotherm, thermodynamic and adsorption-mechanism studies, Clay Miner., 53 (2018) 159–174.
[47] Y.S. Ho, G. McKay (Fellow), Kinetic models for the sorption of dye from aqueous solution by wood, Process Saf. Environ. Prot., 76 (1998) 183–191.
[48] I. Langmuir, The adsorption of gases on plane surfaces of glass, mica and platinum, J. Am. Chem. Soc., 40 (1918) 1361–1403.
[49] H.M.F. Freundlich, Over the adsorption in solution, J. Phys. Chem., 57 (1906) 1100–1107.
[50] K.R. Hall, L.C. Eagleton, A. Acrivos, T. Vermeulen, Pore- and solid-diffusion kinetics in fixed-bed adsorption under constant-pattern conditions, Ind. Eng. Chem., 5 (1966) 212–223.

[51] K. Chinoune, K. Bentaleb, Z. Bouberka, A. Nadim, U. Maschke, Adsorption of reactive dyes from aqueous solution by dirty bentonite, Appl. Clay Sci., 123 (2016) 64–75.
[52] Y. Miyah, M. Idrissi, F. Zerrouq, Etude et Modélisation de la Cinétiqued'Adsorption du Bleu de Méthylène sur les AdsorbantsArgileux (Pyrophillite, Calcite) [Study and modeling of the kinetics methylene blue adsorption on the clay adsorbents (pyrophillite, calcite)], J. Mater. Environ. Sci., 6 (2015) 699–712.
[53] B. Meroufel, O. Benali, M. Benyahia, Y. Benmoussa, M.A. Zenasni, Adsorptive removal of anionic dye from aqueous solutions by Algerian kaolin: characteristics, isotherm, kinetic and thermodynamic studies, J. Mater. Environ. Sci., 4 (2013) 482–491.
[54] S. Banerjee, S. Dubey, R.K. Gautam, M.C. Chattopadhyaya, Y.C. Sharma, Adsorption characteristics of alumina nanoparticles for the removal of hazardous dye, Orange G from aqueous solutions, Arabian J. Chem., 12 (2019) 5339–5354.
[55] E. Errais, J. Duplay, F. Darragi, I. M'Rabet, A. Aubert, F. Huber, G. Morvan, Efficient anionic dye adsorption on natural untreated clay: kinetic study and thermodynamic parameters, Desalination, 275 (2011) 74–81.
[56] M.K. Purkait, A. Maiti, S. Dasgupta, S. De, Removal of Congo red using activated carbon and its regeneration, J. Hazard. Mater., 145 (2007) 287–295.
[57] M. Leu, A. Marciniak, J. Chamberland, Y. Pouliot, L. Bazinet, A. Doyen, Effect of skim milk treated with high hydrostatic pressure on permeate flux and fouling during ultrafiltration, J. Dairy Sci., 100 (2017) 7071–7082.
[58] C. Tansakul, S. Laborie, C. Cabassud, Membrane hybrid processes for pretreatment before seawater reverse osmosis desalination, Desal. Water Treat., 9 (2009) 279–286.
[59] G. Veréb, P. Kassai, E.N. Santos, G. Arthanareeswaran, C. Hodúr, Z. László, Intensification of the ultrafiltration of real oil-contaminated (produced) water with pre-ozonation and/or with TiO_2, TiO_2/CNT nanomaterial-coated membrane surfaces, Environ. Sci. Pollut. Res., 27 (2020) 22195–22205.